

Large-scale Robotic 3D Printing of Plant Fibre and Bioplastic Composites

Christoph Klemmt¹, Mania Aghaei Meibodi², Gregory Beauchage³, Wes McGee⁴

¹University of Cincinnati, Orproject ²DART Lab, Taubman College of Architecture and Urban Planning, University of Michigan ³Department of Chemical and Materials Engineering, University of Cincinnati ⁴Matter Design, Taubman College of Architecture and Urban Planning, University of Michigan

¹christoph@orproject.com

This paper presents a methodology for the robotic 3D printing of cellulose and wood shavings with bioplastics for applications in architecture, moulds, or furniture design. The material composition consists of plant fibre, binders, solvents and additives. All of the ingredients are either biodegradable or biocompatible, as in, they naturally occur in the environment. Different material compositions have been explored and tested for their extrusion behaviour, drying and curing behaviour, buildability and final product qualities, resulting in the manufacture of several case-study prototypes as a proof of concept.

Keywords: 3D Printing, Wood, Cellulose, Bioplastic, Robot, Growth Simulation.

INTRODUCTION

Several conventional construction methods have difficulties to address the current crisis of material scarcity, labour shortage, and the CO₂ footprint resulting from the building industry. Additive manufacturing (AM) can help address these challenges (World Economic Forum 2020). Additive manufacturing, also known as 3D printing (3DP), enables the manufacturing of complex parts with high resolution directly from digital files and raw materials. 3D printing at the scale of architecture and large-scale building components has become a feasible alternative to conventional means of construction. It is expected to significantly increase market share in the coming years (Nematollahi et al. 2017, Parupelli and Desai 2019). Most large-scale 3D printing research for construction has been intensively focused on concrete, metal, and polymers (Hansemann et al. 2020, Buchanan and Gardner 2019, Yu 2017).

This research will expand the field of construction 3D printing by investigating large-scale robotic 3D printing of cellulose and bioplastic composites. Developing 3D printing methods, plant-based material for construction is sustainable, biodegradable, utilises minimal energy, reduces waste, pollution, and costs associated with construction, and creates a more healthy built environment. Based on a review of the state of the art, a production methodology has been developed and tested through different case-studies.

STATE OF THE ART IN 3D PRINTING OF WOOD COMPOSITES

Printing Methodologies

Currently, the production of 3D printing wood biocomposites for construction has been achieved through the following processes: Powder-based and binder jetting technology to 3D print parts from

wood sawdust (Zeidler et al. 2018, Henke and Treml 2013, Rael and San Fratello 2018), Fused Deposition Modeling (FDM) of wood biocomposites filament (Le Dugou et al. 2016), robotic pellet extrusion of 3D granules (Davide 2019), extrusion of a mixture of wood powder and adhesive (Rosenthal et al. 2018, Kam et al. 2019). In Powder-based and binder jetting technology to 3D print parts from wood sawdust, a thin layer of sawdust is spread and bound layer by layer using a nontoxic binder. In Fused Deposition Moulding (FDM) of wood biocomposite, a wood-fill thermoplastic filament is pushed through a heated nozzle that melts the material and deposits it to build parts layer by layer. The wood-fill thermoplastic filament is 70% thermoplastic blended with 30% recycled wood fibres. Robotic pellet extrusion of 3D granules uses a screwing method to melt and transport pelletized wood-based polymer from the barrel through a heated nozzle. Here pellets are fed into a feeder inlet then are pushed through a barrel with multiple heated sections where they are heated to soften. The screw mechanism forces the softened material out through a nozzle onto a heated platform, creating 3D printed parts layer-by-layer. The extrusion process with a mixture of wood powder and adhesive uses different methods to force the material through a container and out of the nozzle.

High Wood Content 3DP

There is limited literature describing high wood-content composites with greater than 85% wood content for 3DP. Compostable but not biodegradable wood-like filaments commercially available are composed of about 70% polylactic acid (PLA) and 30% wood fibre (Le Dugou et al. 2016, Wang et al. 2018). A similar material composition as granules is used for large-scale 3D printing (Davide 2019). Kariz et al. (2016) used polyvinyl acetate (PVAc) and urea-formaldehyde (UF) adhesives as binder with fine wood powder to extrude 3D printed objects. Due to the high viscosity, the wood content was 12–25%. The extrudate had shrinkage of about 20% on curing. Early-stage research has investigated

the small-scale 3DP by extrusion using liquid deposition of fine wood powder with cellulose or lignin binder with 90% wood and up to 100% content of wood products (Rosenthal et al. 2018, Kam et al. 2019). Shrinkage after curing and drying is on the order of 20%.

On a small scale, Meghan Trainor (I-Materialise 2011) adopted a commercial machine for powder-based additive manufacturing of solids using 85% wood powder and synthetic resorcinol-formaldehyde resin as a binder. This was limited to 100 mm demonstration parts. The product has a similar composition but is weaker than particle board since it is not steam pressed. Henke and Treml (Henke and Treml 2013) further expand on powder-based 3d printing through the investigation of various wood products (sawdust / wood chips) and several types of binding agents (gypsum / cellulose / sodium silicate / cement). In this process, the best results occurred with cement as the binder, with chips and cement premixed and deposited, followed by application of a water aerosol, arriving at 70% wood content. Zeidler et al. (2018)] used powder bed 3DP and various binders for different bio-based fibres, with up to 94% wood. The best results were found for polyvinyl alcohol. Rosenthal et al. (2018) used sawdust and methyl cellulose binder with a dry content of 89% wood, and 100% wood products. The extrusion slurry was composed of 90% wood dust and 10% of a 5% methylcellulose water mixture. Drying produced a 20% reduction in linear dimension of the printed part.

3DP of Wood Derivatives

Various complicated processes have been developed using 3DP of wood derivatives. Hausmann developed a solvent exchange method where an aqueous cellulose paste is extruded into a complex shape, solvent exchanged with an organic solvent, infiltrated with a synthetic monomer, polymerized and dried (Hausmann et al. 2019). This process led to high resolution, shape-retaining wood-based objects with about 30% wood. Direct cryo-writing involves freezing an aqueous

suspension of cellulose or other wood-based materials during 3d printing. The process has been proposed as a method to generate highly oriented fibres (Deville et al. 2006). The printed object is placed in a vacuum and freeze-dried to remove water by sublimation (Kam et al. 2019). Liangbing Hu at the University of Maryland (Jiang et al. 2020) has developed a process using lignin and triblock Pluronic that can crosslink lignin molecules forming a shear-thinning gel in water. The extrudable gel is an effective 3DP ink and can be used at room temperature. Water is removed from the product by freeze drying resulting in 90% wood-based 3D objects. None of these more complex approaches for 3DP of wood can be used to produce large-scale objects. Most are much too expensive or are not currently possible on a large scale.

Assessment

Due to limitations in affordability, scale, and available materials, additive manufacturing has so far only found limited use in building applications. 3DP processes based on plant fibre mostly exist at the small scale, or with a limited percentage of fibre. This research therefore addresses the lack of large-scale biodegradable 3DP methods with a high percentage of wood content, as well as concerns of a high energy consumption, a limited possible volume fraction of added fibre, extrusion thickness and speed constrained by the cooling rate, and high component weight.

LARGE SCALE EXTRUSION BASED 3D PRINTING PLANT FIBRE

This research presents new 3DP processes based on wood shaving and cellulose that are sustainable, biodegradable, and utilise minimal energy in their production. The objective is to investigate the potential and challenges of robotic extrusion with plant fibre for the construction and production of large building parts. The aim is an understanding of the relationship between material compositions, fabrication setup, design and buildability.

We present a methodology for the robotic 3D printing of wood shavings or cellulose and bioplastics. The material composition consists of plant fibre, a binder, a solvent, and additives. All of the ingredients are either biodegradable or biocompatible, as they naturally occur in the environment. Ingredients that are only industrially compostable such as Polylactic Acid (PLA) have been excluded. The materials are therefore not thermosetting but cured after their extrusion. Different material compositions have been explored and tested for their extrusion behaviour, drying and curing behaviour and final product qualities.

CASE STUDIES

The case studies presented in this paper investigated the challenges and potential of large-scale extrusion-based 3d printing of wood shaving and cellulose. Fabrication setup, material compositions and geometry design are explored to define their relationships in achieving buildability with minimum deformation. Some of the prototypes were produced in academic seminars.

Fabrication Setup

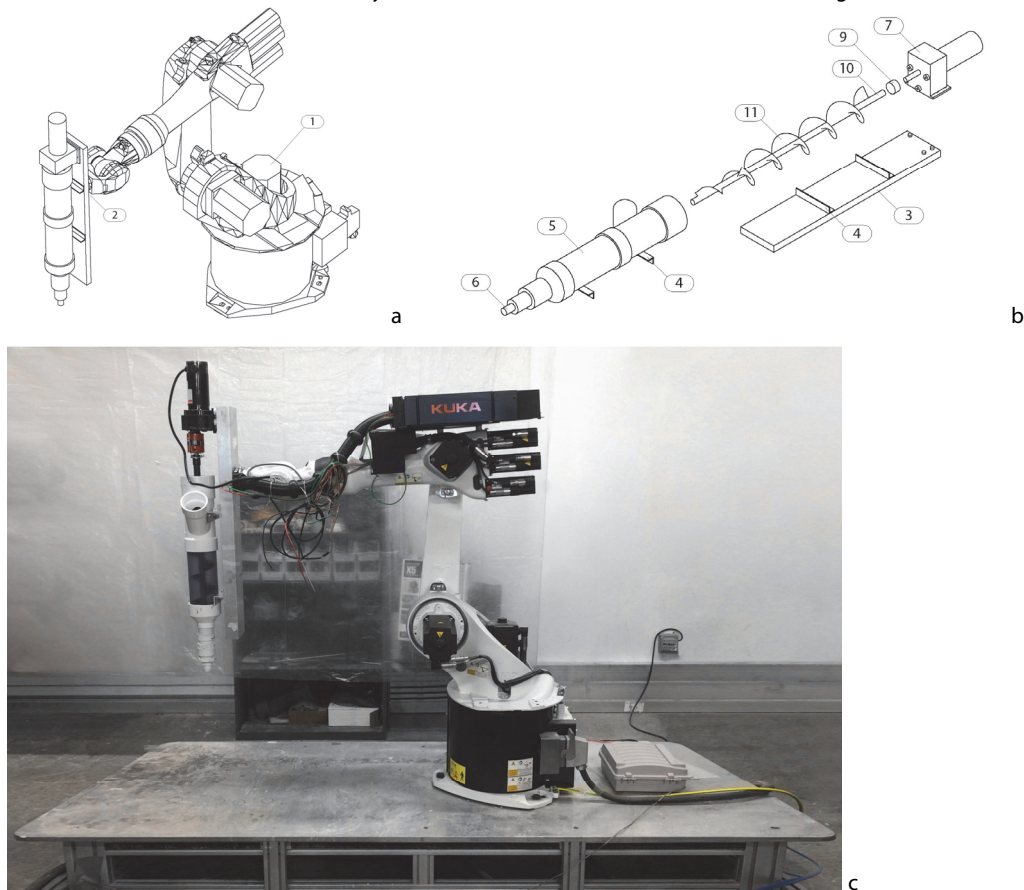
Two extruders were used for the prototypes presented in this paper. The cellulose-based slurries were extruded with a commercially available clay extruder (VormVrij Lutum Bronze Extruder V6). At the same time, a custom system was constructed for the compositions with the larger wood shavings (Figure 1). This extrusion setup is aimed at large scale architectural applications and therefore requires the possibility of a continuous material flow rate. At the current extruded bead dimensions of approximately 30mm width and 10 mm thickness, this translates to a volumetric flow rate of 1L – 2L per minute, corresponding to robotic motion of 50mm – 100 mm/s along the path. In order to maintain a continuous and controllable flow, a positive displacement extrusion system is ideal as its flow rate is directly proportional to its speed and number of cycles over a given time. The simplest positive displacement system is piston driven, however this

functions as a closed system that requires an interruption of the extrusion process for the refilling of the chamber. Therefore an auger-feeding system was utilised for the prototypes of this paper that allows for a continuous refilling during the extrusion process. While screw type augers are not positive displacement, they are simpler and cheaper to build than more advanced systems such as progressive cavity pumps. The auger is positioned within a PVC pipe assembly that is attached to a vertical aluminium base, driven by a motor from above.

The material, after its initial preparation, is likely to have inconsistencies in its density due to air

pockets, and the extruder was intended to handle a discontinuous feed of the input material so that its refilling during the extrusion process can happen at irregular intervals. The system therefore needs to compact the material to remove any enclosed air and to generate a continuous output feed. This was achieved via a three-step auger system that decreases in its diameter and therefore its flow rate progressively through the assembly. The auger starts with an initial diameter of 100mm that reduces down to 50mm, and then further to 25mm. The 25mm diameter section of the auger is positioned within the area of the exchangeable nozzle, with

Figure 1
Auger-actuated
Extruder Assembly
and Robotic Set-up.



opening diameters of 40mm, 25mm and 19mm. The width of the extruded material is wider than the size of the nozzle.

The extruder can hold approximately 6l of material and is refilled via a sideways input at the top of the assembly. For this project the extruder was refilled manually, however for the next prototype iteration with high volume of material refilling will be achieved via a pump. As larger wood particles can become lodged between the auger and its PVC chamber, a high-torque DC motor is required to drive the auger. Also, the spacing between the auger and the chamber needs to be large, in our case about 5mm, to prevent the lodging of the particles.

A Kuka KR20-3 was used for the motion control of both extruders, programmed via the Rhino / Grasshopper / KukaPRC plug-in.

Extruder Assembly:

- 1) Robot: KUKA KR20-3 with controller KR C4
- 2) Manual Tool Changer: Millibar MTC-UR3510
- 3) Extruder Frame: Aluminium RHS, 125mm x 50mm x 3mm
- 4) Brackets: Aluminium Angles, 40mm x 40mm x 3mm
- 5) Chamber PVC pipes: 100mm x 100mm x 50mm Wye, 100mm x 300mm clear pipe, 100mm x 50mm reducer hub, 50mm x 100mm pipe, 50mm x 40mm/25mm reducer hub
- 6) Nozzle PVC pipes: exchangeable nozzles at 40mm / 25mm / 19mm diameter
- 7) Motor: Dayton Model 1Z824 DC Gear Motor 50 RPM 1/6 hp 12VDC
- 8) Power Supply: eTopxizu 12v 30a Dc Universal Regulated Switching Power Sup-ply 360w
- 9) Coupling: Lovejoy L099 HUB, keyed flexible shaft coupling 16mm/19mm
- 10) Connector: Steel Rod 19mm diameter
- 11) Auger: custom designed three-step auger: 100mm diameter, 50mm diameter, 20mm diameter

Material Composition

As the project aims for sustainable material compositions, all fibres, binders, solvents and

additives are chosen to be either biodegradable, or to be abundant in nature such as silica.

Two types of fibre were utilised in the experiments: cellulose, with 75% softwood and 25% hardwood fibres, and wood shavings with approximate dimensions of 1-5mm x 5-30mm. Different types of bioplastics and solvents were explored, however, most compositions had a significant water content. A high percentage of binders and solvents was required to ensure that the fibres did not clog the extruder. This resulted in a low viscosity material and required a drying time on the order of several days, which in turn restricted buildability –the ability to 3D print continuously to the required level without significant deformation or collapse of the freshly printed component.

To address the viscosity, plasticity and drying behaviour, different additives were included in the compositions.

Computational Design

The current viscosity of the material compositions, as well as its slow drying time, required printing geometries that are relatively stable at every point during their extrusion, and that therefore only have minor overhangs. Several geometries to print were therefore generated by means of a 2D Differential Growth simulation (Lomas 2014, Louis-Rosenberg 2015). The algorithm is based on a 2D closed curve that is divided into evenly spaced nodes $V_i, i = 1 \dots k$, for the examples of this paper at an approximate distance of 0.2. In each iteration of the growth logic, the nodes move and reposition according to their neighbours, and further nodes are inserted between two neighbours if their distance exceeds a given threshold. The curve thereby continuously increases in its node count and expands, commonly leading to a folding of its geometry. The algorithm was scripted in Python using the Rhino/Grasshopper environment. The following basic behaviours have been programmed to guide the repositioning of the nodes:

Figure 2
 Toolpath generated by the Differential Growth algorithm, showing the waving of the geometry and the limited overhangs. This toolpath was used in the prototype of Figure 3b.

Spring Force

The spring force is based on Hooke's Law and acts between a node P and its two neighbouring nodes N_1, N_2 along the curve. It is based on a given restlength rl , the distance that a node attempts to achieve towards a neighbour. The Spring Force therefore makes the node move along the direction towards its neighbour, with its strength related linearly to the deviation of the actual distance of the two nodes in relation to the rest length. Common values for the simulations of this paper were a rest length of 0.2, and a multiplying factor of 0.1.

$$force_{Spring} = factor_{Spring} * \sum_{j=1}^2 \overrightarrow{N_j - P} * |rl - |N_j - P|| / |N_j - P| \quad (1)$$

Smooth Force

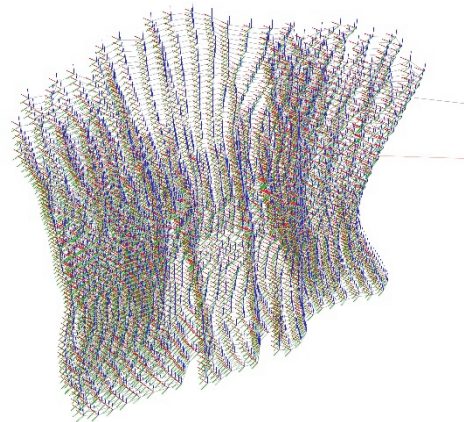
The smooth force attempts to align adjacent nodes, thereby reducing sharp corners and creating a smoother curve. The force acts by finding the midpoint of a node's two neighbours and pulling the node towards this midpoint. A common multiplying factor for the simulations of this paper was 0.25.

$$force_{Smooth} = factor_{Smooth} * ((N_1 + N_2) * 0.5 - P) \quad (2)$$

Point Force

A repelling point force is calculated for non-neighbouring nodes that are within a given range of influence distance roi from each other. This force ensures that nodes other than the direct neighbours are pushed away to prevent a self-intersection of the curve. This then leads to the folding and bulging out of the curve geometry. A common multiplying factor for the simulations of this paper was 0.005, with an roi of 0.4.

$$force_{Point} = factor_{Point} * \sum_{i=1}^k \frac{\overrightarrow{V_i - P}}{|V_i - P|^2} if (|V_i - P| < roi) if not(V_i \in (N_1, N_2, P)) \quad (3)$$



The three forces are added to find the movement vector of a node in each iteration. Additional forces that relate to objects positioned around the curve can be incorporated, and the possible positions of the nodes can be constrained to a given geometry. Lastly, new nodes are inserted centrally between any two neighbouring nodes that exceed a given distance, in the simulations of this paper set to 0.15.

This growth logic results in the given curve expanding continuously, while creating folds in many areas. The curves from each iteration of the simulation are then stacked vertically, starting with the final curve of the simulation as the lowest of the geometry to print. In this way, the curves can directly be used as the robotic toolpath, with the inclinations controlled by the growth simulation (Figure 2).

RESULT AND DISCUSSION

Several prototypes were extruded with both wood shavings (Figure 3) as well as cellulose fibres (Figure 4). For all material compositions, the printing height was limited. The compositions with wood shavings could be printed to a height of about 300mm, while the compositions with cellulose had a limit of about 100mm. Above this, the buildability was impacted by the relatively low viscosity of the extrudate, which resulted in significant deformations or a collapse of

Figure 3
 Extrusions with
 Wood Shavings of
 up to 2m in length.
 Toolpath of
 prototype b is
 shown in Figure 2.
 Projects c-e by
 Josiah Ebert, Jinhui
 Huang, Tyler
 Kennedy, Brandon
 Kroger, Jianna Lee,
 Drew Pederson,
 Robert Peebles,
 Tess Ryan.



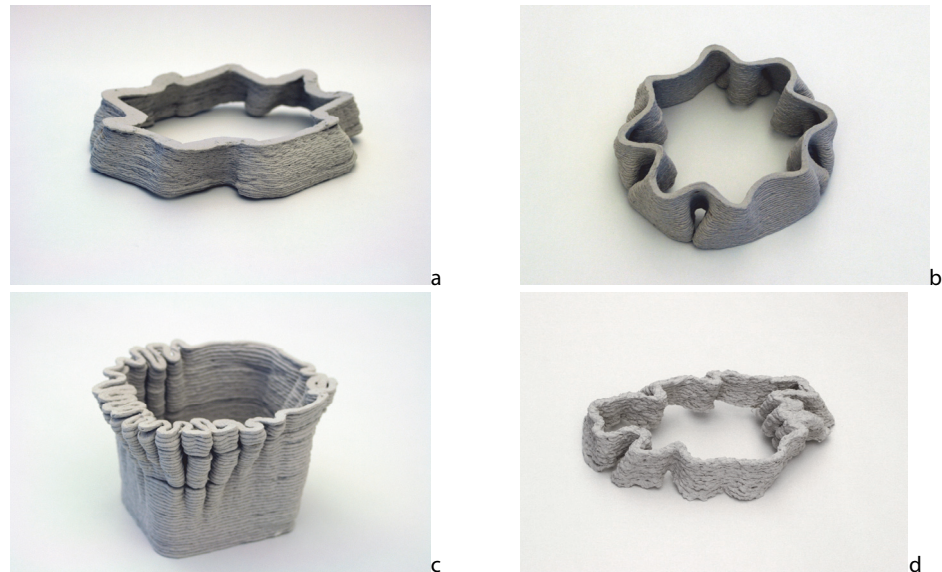
the structure. Separately extruded sections can be stacked as in Figure 03b.

Significant shrinkage was observed, especially in the extrusions with cellulose. This resulted either in warping of layers that were horizontal at extrusion, as in Figure 04 a, b, and d, or that led to inter-layer separations, as in Figure 04c. Especially the 3DP with wood shavings led to a rough surface finish. Post-processing, such as sanding, led to a clear improvement of the smoothness, as in Figure 03e.

Material Composition

Compared to existing materials, our composition allows for a biodegradable material for large-scale applications, although at lower resolution. While the material compositions allowed for an extrusion of plant-based fibre, further development is needed to address the currently limited printable height, stability after extrusion, shrinkage, and possibly surface finish. The main concern is the relationship between solvent and binder content with its corresponding viscosity and the relating extrudability, curing and drying time, which define

Figure 4
Extrusions with Cellulose, up to 150mm in height. Shrinkage is visible in the horizontal warping of the planar extruded layers. Projects by Andrew Clark, Brendan Girten, Daniel Gonzalez, Evan Hammans, Hang Phan.



the possible printing height. As the fibre content increases, extruder clogging becomes more likely, as the binder and solvent not only act to connect the fibres in the final piece, but also act as the slurry that transports the fibres through the extruder. The large amount of solvent then leads to a low viscosity of the extrudate, which leads to limited buildability and shrinkage. While with the current compositions, several layers of extrudate can easily be stacked upon each other, at a certain height the material becomes less stable and eventually collapses.

In order to address this, future work will explore the possibilities of other additives for rheology control, and other possible solvents. Specific consideration should be given to possible curing additives that can result in a rapid setting soon after the extrusion of the material, so that the viscous extrudate is stabilised to support further printing layers above.

Extrusion System

The extrusion system was able to extrude the developed material compositions. However, tests with larger wood pieces led to a blockage of the

system. Also, a slight soaking of the wood shavings made them more flexible and reduced the possibility of clogging.

In order to improve the control and efficiency of the material delivery, future research will explore the use of a two-stage pumping system, which has been shown to be effective with other fibrous paste materials such as engineered cementitious composite (Mcgee, 2020). A two-stage system allows for the continuous delivery of either batch or continuously mixed, de-aired material to a robot-mounted extruder. Such a system can be used with higher viscosity pastes, allowing the improvements to the material discussed above, and can also be adapted to include mixing stages for rheology control near the point of the extrusion.

Computational Design

The Differential Growth algorithm succeeded in limiting overhang and generating extrudable tool paths. Especially the waving of the resulting surfaces created stable structures. Collapse occurred in some prototypes in those areas that were mostly straight with limited waving. Collapse also occurred in areas

with a significant overhang above 15° that was not supported by waving or orthogonally positioned material.

CONCLUSIONS

In order to address the extensive CO₂ emissions of the construction industry, significant changes are required to the building methods that we utilise. The proposed methodologies of 3D-printing with wood, cellulose and bioplastics are addressing those needs through renewable resources, biodegradability, and low energy consumption of the production processes. The materials have successfully been used to extrude prototypes at small and medium scales of up to 300mm in height. While this constitutes a proof of concept, adjustments especially of the material compositions are required to improve buildability and shrinkage.

REFERENCES

- Buchanan, C; Gardner, L. 2019. Metal 3D printing in construction: A review of methods, research, applications, opportunities and challenges. *Eng. Stru.* 180 332–348.
- Davide, S. 2019. UPM demonstrates large scale robotic 3D printing of wood polymer composites.[online] Available at: <https://www.3dprintingmedia.network/upm-demonstrates-large-scale-robotic-3d-printing-of-wood-based-polymer-composites/> (accessed on 10/5/2020).
- Deville, A; Saiz, E; Nalla, RK; Tomsia, AP. 2006. Freezing as a Path to Build Complex Composites *Science* 311 515–518.
- Hansemann, G; Schmid, R; Holzinger, C; Tapley, J; Kim, H; Sliskovic, V; Freytag, B; Trummer, A; Peters, S. 2020. Additive Fabrication Of Concrete Elements By Robots: Lightweight Concrete Ceiling. In *Fabricate 2020: Making Resilient Architecture* Eds. Burry, J; Sabin, JE; Sheil, B; Skavara, M 124-129. UCL Press, London.
- Hausmann, MK; Siqueira, G; Libanori, R; Kokkinis, D; Neels, A; Zimmermann, T; Studart, AR. 2019. Complex-Shaped Cellulose Composites Made by Wet Densification of 3D Printed Scaffolds *Adv. Funct. Mater.* 30 201904127. <https://doi.org/10.1002/adfm.201904127>
- Henke, K; Tremi, S.2013. Wood based bulk material in 3D printing processes for applications in construction *Eur. J. Wood Prod.* 71 139–141.
- I-Materialise. 2011. 3d Printing in Wood Flour. [online] Available at: <https://i.materialise.com/blog/en/3d-printing-in-wood-flour/> (accessed 8/8/2020)
- Jiang, B; Yao, Y; Liang, Z; Gao, J; Chen, G; Xia, Q; Mi, R; Jiao, M; Wang, X; Hu, L. 2020. Lignin-Based Direct Ink Printed Structural Scaffolds *Small* 16 201907212. <https://doi.org/10.1002/smll.201907212>
- Kam, D.; Layani, M; Minerbi, SB; Orbaum, D; Ben Harush, SA; Shoseyov, O; Magdassi, S. 2019. Additive Manufacturing of 3D Structures Composed of Wood Materials *Adv. Mater. Technol.* 4 1900158. <https://doi.org/10.1002/admt.201900158>
- Kariz M, Sernek M, Kitek Kuzman M. 2016. Use of wood powder and adhesive as a mixture for 3D printing. *Eur. J. Wood Prod.* 74 123–126.
- Le Duigou A, Castro M, Bevan R, Martin N. 2016. 3D printing of wood fibre biocomposites: from mechanical to actuation functionality. *Mater. Des.* 96 106–114.
- Lomas, A. 2014. Cellular Forms: an Artistic Exploration of Morphogenesis. in ACM SIGGRAPH Studio.
- Louis-Rosenberg, J. 2015. Floraform – An Exploration of Differential Growth. [Online]. Available: <http://n-e-r-v-o-u-s.com/blog/?p=6721> (accessed May 17 2017)
- McGee, W; Ng, TY; Li, VC; Yu, K. 2020. Extrusion Nozzle Shaping as an Approach for Improved 3DP of Engineered Cementitious Composites (ECC/SHCC). *Digital Concrete 2020*. Springer, New York.
- Nematollahi, B; Xia, M; Sanjayan J. 2017. Current progress of 3D concrete printing technologies. ISARC. In *Proceedings of the International Symposium on Automation and Robotics in*

- Construction 34 260-267 IAARC Publications, New York.
- Parupelli, SK; Desai S. 2019. A comprehensive review of additive manufacturing (3d printing): Processes, applications and future potential. Am. J. Eng. Appl. Sci. 16 244-27.
- Rael, Ronald, and San Fratello, Virginia. 2018. Printing architecture: Innovative recipes for 3D printing. Chronicle Books
- Rosenthal, M; Henneberger, C; Gutkes, A; Bues CT. 2018. Liquid Deposition Modeling: a promising approach for 3D printing of wood Eur. J. Wood Wood Prod.76 797–799.
- Wang Q., J. Sun, Q. Yao, C. Ji, J. Liu, Q. Zhu. 2018. 3D printing with cellulose materials Cellulose. 25:4275–4301.
- World Economic Forum. 2020. CO2 can help the construction industry emit less CO2. Here's how. [Online]. Available at: <https://www.weforum.org/agenda/2020/12/co2-can-help-the-construction-industry-thrive-heres-how/>(accessed 10th January 2021)
- Yu, L. 2017. Arachne - A 3D-Printed Building Facade. In Projects Catalog of the 37th Annual Conference of the Association for Computer Aided Design in Architecture. Boston. Eds. Lamere J; Alonso, CP 280-285 ACADIA.
- Zeidler, H; Klemm, D; Böttger-Hiller, F; Fritsch, S. 2018. 3D printing of biodegradable parts using renewable biobased materials Procedia Man. 21 117–124.